RSC Advances

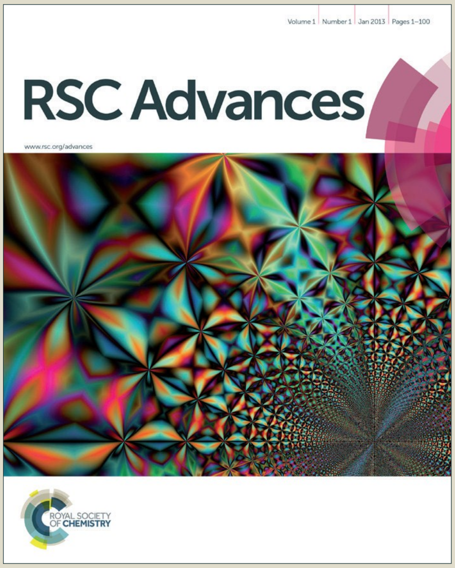

ROYAL SOCIETY OF CHEMISTRY

www.rsc.org/advances

RSC Advances RSCPublishing

ARTICLE

Cite this: DOI: 10.1039/x0xx00000x

Received,
Accepted

DOI: 10.1039/x0xx00000x

www.rsc.org/

Synthesis of copper(II) complex covalently anchoring (2-iminomethyl)phenol moiety supported on HAp-encapsulated-α-Fe_2O_3 as an inorganic–organic hybrid magnetic nanocatalyst for the synthesis of primary and secondary amides

M. Mamaghani*, F. Shirini, M. Sheykhan, M. Mohsenimehr

A novel hydroxyapatite-encapsulated-α-Fe_2O_3-based Cu(II) organic-inorganic hybrid (interphase) catalyst was prepared. The prepared nanocatalyst provided an efficient, useful and green method for the oxidative amidation of the aromatic aldehydes with ammonium hydrochloride and aniline hydrochloride, in short reaction times and good yields. Magnetic nature of the catalyst led to its easy recovery by an external magnetic field and convenient reuse.

Introduction

Homogeneous catalysts have some advantages due to their uniform and well defined reactive centres which lead to their high activity and selectivity. Also, homogeneous catalysts allow for more effective mixing of the catalyst with the reaction mixture (occupy the same phase as the reactants), which in turn creates problems of catalyst separation from the reaction mixture and therefore the catalyst is difficult to reuse. To solve this problem, several methods have been checked out to combine the advantages of homogeneous and heterogeneous catalysis.[1] In this respect, nanoparticles (NPs), especially magnetic NPs (MNPs) have appeared as a bridge between homogeneous and heterogeneous catalysts. The magnetic nature of these particles allows for easy recovery (green chemistry) and recycling of the catalysts by an external magnetic field.[2] To improve the chemical stability as well as to achieve some advantages as the versatility in surface modification, MNPs commonly coat with different organic or inorganic compounds, precious metals and recently calcium hydroxyapatite $Ca_{10}(PO_4)_6(OH)_2$ (HAp).[3]

Covalently combining an active site onto a large surface area solid through a flexible spacer to create an organic-inorganic hybrid (interphase) catalyst is known as a way to simulate homogeneous reaction conditions together with having the advantage of recyclability.[1,4,5]

On the other hand, amide bonds have been found in many natural important polymers such as peptides and proteins and in a wide range of biological compounds, such as pharmaceuticals and is also employed as synthetic intermediates for fine chemical industry and agrochemicals.[6,7] Commonly, the amide bond is synthesized by acylation of amines with either activated carboxylic acids or coupling with carboxylic acids mediated by a coupling reagent.[8,9] However, these methods have the innate problems of producing waste products, use of hazardous reagents and poor atom economy.[10] To solve these problems in amide synthesis, novel methods were developed, such as direct amide synthesis from alcohols with amines or nitroarenes,[11] amino carbonylation of haloarenes,[12] hydroamination of alkynes, amidation of thioacids with azides,[13] transamidation of primary amides,[14] and C–H oxidative amidation.[15]

Among these, oxidative amidation of aldehydes with amine salts is synthetically useful and less hazardous than those traditionally used such as acid halides, which was first reported by Nakagawa et al. in 1966 using stoichiometric amounts of nickel peroxide as the oxidant.[16] Subsequently, other researchers have used new oxidants and novel catalysts for the direct conversion of aldehydes to amides.

More recently, Yoo and Li introduced a copper-catalyzed procedure for oxidative amidation of aldehydes with amine hydrochlorides using CuI−$AgIO_3$ as the catalyst and *tert*-butyl hydroperoxide as the oxidant.[17]

In the years since, other copper catalysts such as $Cu(OAc)_2$ and $CuSO_4.5H_2O$ have been reported for the amidation reactions.[18] Silica-coated magnetic carbon nanotubes (MagCNTs@SiO_2)-immobilized imine–Cu(I) was also introduced as a magnetic heterogeneous catalyst for the synthesis of different types of amides.[19] Although, significant advances have been achieved in this field, but introduction of an efficient, economical and greener catalyst is still desirable.

On the basis of the above concerns, we report herein a novel copper(II) complex covalently anchoring (2-iminomethyl)phenol moiety supported on HAp-encapsulated-α-

Fe_2O_3 (denoted as catalyst **4**) (Scheme 1) as an inorganic-organic hybrid magnetic nanocatalyst for efficient oxidative amidation of aromatic aldehydes with amine hydrochloride and aniline hydrochloride.

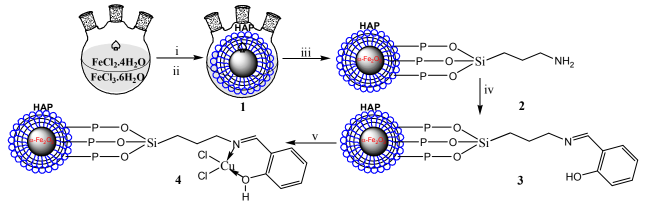

Scheme 1. i) $Ca(NO_3)_2$, $(NH_4)_2HPO_4$, NH_4OH, ii) calcination, iii) 3-aminopropyltrimethoxysilane, toluene, reflux, 48 h, iv) 2-hydroxy benzaldehyde, dry EtOH, reflux, 24 h, v) $CuCl_2$, EtOH, r.t., 12 h.

Results and discussion

In continuation of our research devoted to the development of new benign methodologies for the preparation of magnetic nanoparticles,[3a,20] we were interested in the synthesis of amide derivatives using nanocatalyst **4** (Scheme 1). The magnetic nanoparticles (Fe_3O_4) were synthesized by a chemical co-precipitation technique using ferric and ferrous ions. Based on our previous report,[3a] after coating a layer of hydroxyapatite on the surface of the Fe_3O_4 nanoparticles and its calcination at 450°C, it was functionalized by 3-aminopropyltrimethoxysilane to produce an organic–inorganic hybrid. Then, the prepared hybrid was reacted with 2-hydroxybenzaldehyde to obtain a bi-dentate ligand functionalized core-shell magnetic nanocatalyst (named as catalyst **3**). Finally, surface-bound ligands were complexed with copper(II) by using $CuCl_2$ (Scheme 1). The nanocatalyst **4** was characterized by various microscopic and spectroscopic techniques such as XRD, FT-IR, ICP, SEM-EDX, VSM. In the FT-IR spectrum (Fig. 1), the absorption peak at 464 cm^{-1} can be assigned to the Fe-O absorption in the hematite.[21] The O–P–O surface phosphate groups in the hydroxyapatite shell appeared at 570 and 604 cm^{-1} which were in overlap with Fe–O stretching. Also, the P–O stretching appeared at 1040 cm^{-1}. Signals at around 1419 and 1458 cm^{-1} related to the aromatic C=C stretching as well as a signal at 1629 cm^{-1} produced by C=N double bond confirm that the organic linker was properly immobilized onto the surface. Note that the C=N signal is shifted to a lower wavenumber than the C=N stretching frequency of **3** (1629 cm^{-1} rather than 1634 cm^{-1}). It is implying that C=N bond is coordinated to copper through the lone pair of nitrogen and oxygen. In XRD analysis (Fig. 2), the resulted patterns can be readily referred to α-Fe_2O_3 (JCPDS no. 33-0664), and hydroxyapatite (JCPDS no. 24-0033). Diffraction peaks at around 28.0°, 38.6°, 41.6°, 47.8°, 58.0°, 63.6°, 66.8°, 68.0°, 72.8° and 74.2° correspond to the (012), (104), (110), (113), (024), (116), (122), (018), (214) and (300) reflections patterns of hematite. No other phase except the hematite and hydroxyapatite is detectable. The measurements were carried out on a Philips X'Pert diffractometer with Co*Kα* radiation. The ICP analysis showed that 4.9% of Cu was anchored on catalyst 4. It means that there is about 0.8 mmol (Cu) per gram of the catalyst.

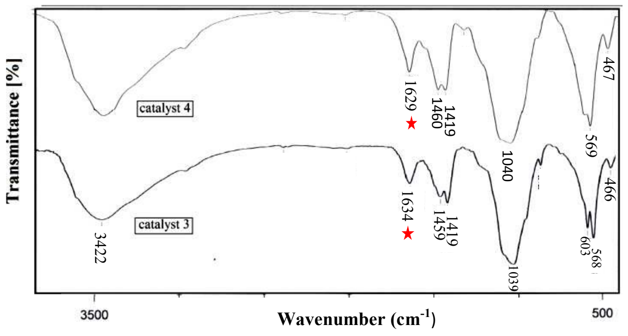

Fig. 1. FT-IR spectrum of catalysts **3** and **4**

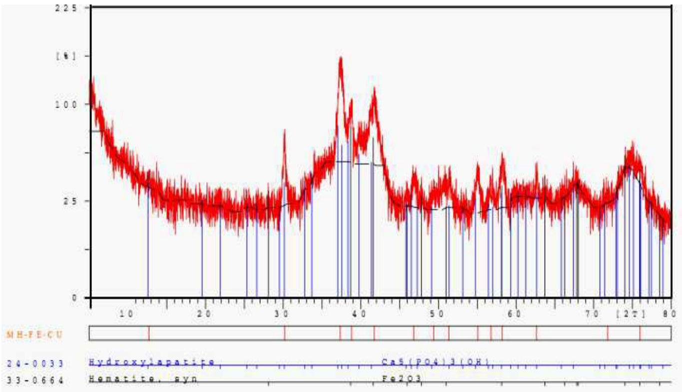

Fig.2. XRD spectra of catalyst 4

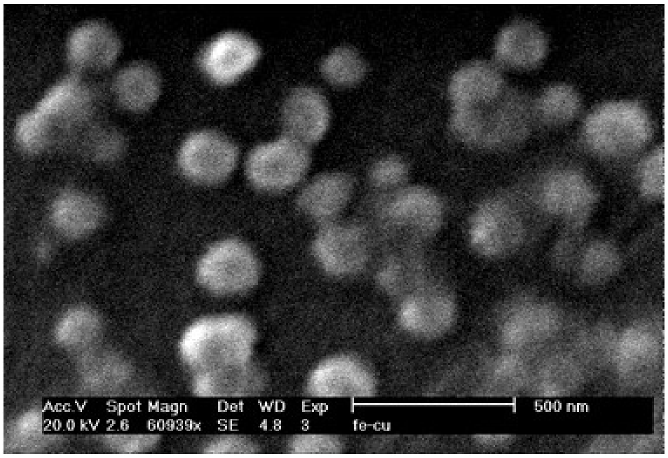

Fig. 3. SEM image of catalyst **4**

The morphology and size details were investigated by SEM measurement (Fig. 3). The SEM image of the catalyst clearly showed the nano size of the particles (with an average about 50 nm) and their morphology is spherical. The SEM image of the catalyst taken after the fifth cycle of the reaction did not show significant change in the morphology or in the size of the catalyst nanoparticles (58 nm) (Fig. 4), which indicates the retention of the catalytic activity after recycling.

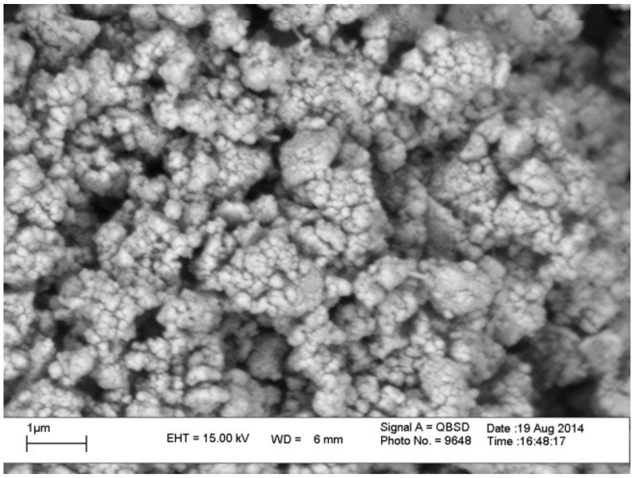

Fig. 4. SEM image (after the fifth cycle of the reaction) of catalyst **4**

The EDX spectrum of the nanocatalyst is presented in Fig. 5, atoms such as Fe, Si, Ca, P, Cu and Cl related to the catalyst structure, are seen in the spectrum. Based on the EDX spectrum the copper:chlorine:nitrogen content of the catalyst were found to be in ratio of 1.2 : 2.03 : 1.0.

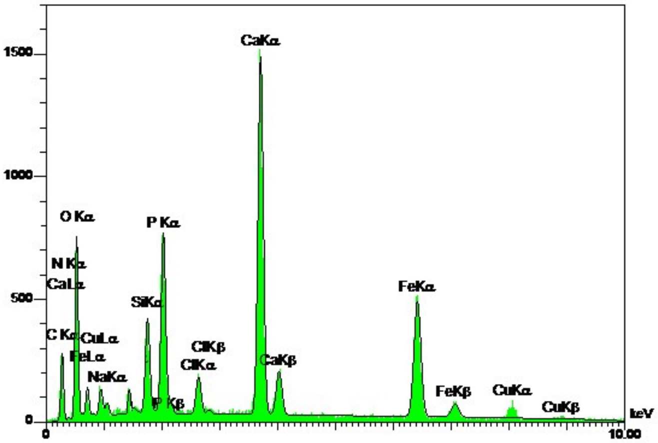

Fig. 5. EDX spectra of catalyst **4**

Magnetic characterization of the nanoparticles, which accounts for its easy recovery, was done using a vibrating sample magnetometer (VSM) at room temperature, with the field sweeping from -8500 to +8500 Oersted. The M(H) hysteresis loop for the sample was completely reversible and the ratio of magnetic remanence (Mr)/magnetic saturation (Ms) is about 0.0005, Ms=3.71 emu.g^{-1}, showing that the nanoparticles exhibit superparamagnetic characteristics (Fig. 6).

After characterization, catalytic activity of the catalyst was tested in the oxidative coupling of the aromatic aldehydes with ammonium chloride and aniline hydrochloride. In a preliminary experiment the reaction of *p*-chlorobenzaldehyde and ammonium chloride was chosen as a model reaction for amidation of aromatic aldehydes and the reaction conditions, such as temperature, reaction time, oxidant and molar ratio of the catalyst to substrate was optimized (Table 1). We found that the reaction of *p*-chlorobenzaldehyde (1 mmol), ammonium chloride (2 mmol) and *tert*-butylhydroperoxide (TBHP) (0.4 mL) as oxidant in CH_3CN (1 mL) in the presence of nanocatalyst (10 mg, 0.8 mol%) and Na_2CO_3 (2 mmol) as base, at 50°C under Ar atmosphere, produce the desired primary amide **5a** in 40 min and 78% yield (Table 1, entry 1). As shown in Table 1, entry 1, TBHP, based on the reaction time and yield, was proved as selected oxidant at 50°C. In comparison, the reaction at room temperature resulted in a pronounced reduction in the yield of product **5a** and increasing the reaction time did not change the efficiency of the reaction significantly (Table 1, entry 4).

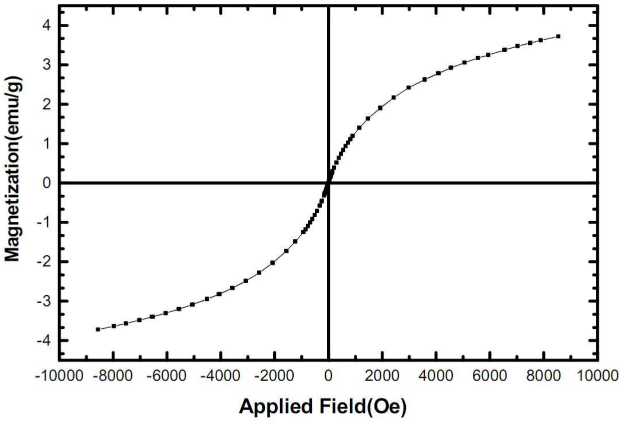

Fig. 6. VSM curve of catalyst 4.

The oxidation efficiency of TBHP was also compared against H_2O_2 (Table 1, entry 2), and the effect of various solvents was examined (Table 1). The results revealed that TBHP in CH_3CN produce a better result and in most of the cases it is not necessary to use the chromatographic methods for separation of the products.

The procedure led to a green method for the synthesis of primary and secondary amides (**5a-k**, **6a-e**, Scheme 2, Table 2).

Table1. Optimization of reaction conditions for synthesis of 4-chlorobenzamide in the presence of nanocatalyst **4.**

Entry	Oxidant	Solvent	Temperature (°C)	Yield (%)[a]	Time (min)
1	TBHP	CH_3CN	50	78	40
2	H_2O_2	CH_3CN	50	50	40
3	TBHP	CH_3CN	r.t.	40	40
4	TBHP	CH_3CN	r.t.	45	90
5	TBHP	CH_3CN	r.t.	45	120
6	TBHP	H_2O+CH_3CN(1:1)	50	39	40
7	TBHP	THF	50	47	40
8	TBHP	DMF	50	24	40
9	TBHP	Toluene	50	54	40

[a] Isolated yield. [b] Reaction conditions: *p*-chlorobenzaldehyde (1 mmol), ammonium chloride (2 mmol), nanocatalyst **4** (10 mg, 0.8 mol%), solvent (1 mL), Na_2CO_3 (2 mmol), oxidant (0.4 mL.), Ar atmosphere.

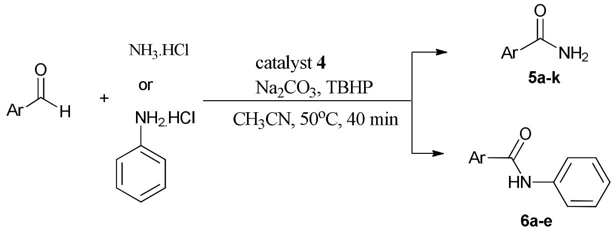

Scheme 2. Synthesis of amide derivatives in the presence of nanocatalyst **4.**

As shown in the Table 2, aromatic aldehydes having both electron-donating and electron-withdrawing groups were converted to the related amides in good yields. Also in some cases the yield of secondary amides is slightly higher than the primary amides.

Reusability of the catalyst was also re-checked in the preparation of **5a**. After completion of the reaction, the nanocatalyst was separated from the reaction medium simply by an external magnetic field, washed with ethyl acetate, dried under vacuum and reused for the next run. After 5 successive runs the catalytic activity of the catalyst was almost remained unchanged (Fig. 2).

Table 2. Synthesis of amide derivatives

Entry	Ar	Product	Yield (%)^{a,b}	m.p.
1	4-ClC_6H_4	5a	78	177-179 [16]
2	4-$HOCC_6H_4$	5b	76	178-181
3	Thiophen-2-yl	5c	77	126-128 [22]
4	4-CNC_6H_4	5d	76	146-148 [22]
5	Cinnamaldehyde	5e	75	147-149 [22]
6	4-FC_6H_4	5f	77	138-140 [22]
7	4-BrC_6H_4	5g	78	192-194 [18]
8	4- $H_3COC_6H_4$	5h	75	165-167 [18]
9	3-$O_2NC_6H_4$	5i	75	141-143 [22]
10	C_6H_5	5j	77	128-130 [24]
11	4-$CF_3C_6H_4$	5k	74	189-191 [18]
12	4-ClC_6H_4	6a	83	192-193 [23]
13	4-BrC_6H_4	6b	84	204-206 [23]
14	C_6H_5	6c	81	164-166 [23]
15	Thiophen-2-yl	6d	79	178-180
16	2,4-$Cl_2C_6H_3$	6e	80	199-201

^{a}Isolated yield, ^{b}Reaction times 40-42 min, [ ] reported references.

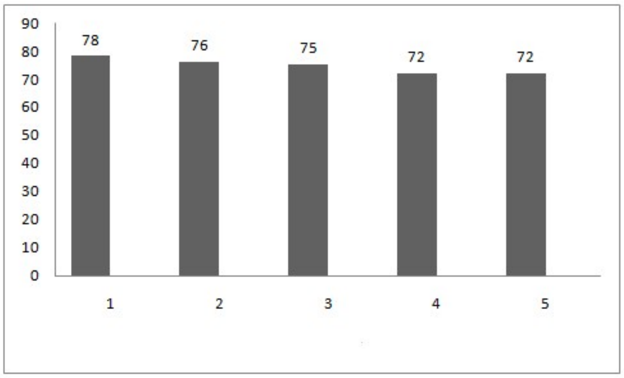

Fig. 2. The reusability of the catalyst **4** in five runs for the preparation of compound **5a**.

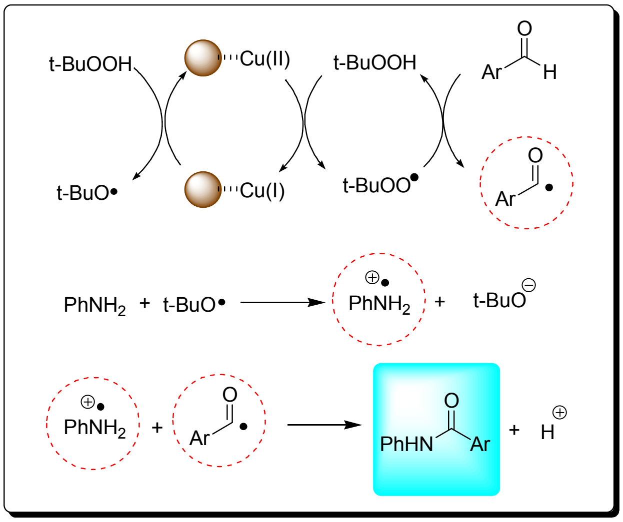

Scheme 3. The Postulated mechanism for the catalytic amidation in the presence of the catalyst **4**

On the basis of the reaction conditions, we propose that in the first step (Scheme 3) catalyst **4** reacts with TBHP generating a *tert*-butylperoxy radical following the mechanism proposed in literature [25] and a Cu(I)–anchored on the catalyst surface is re-oxidized by another TBHP. The aniline hydrochloride is then converted into an amino radical by the resulting *tert*-butyloxy radical. The reaction between aldehyde and *tert*-butylperoxy lead to an acyl radical, as reported previously.[26] Finally, a terminative coupling reaction occurs between the acyl radical and the amino radical to form the desired amide. To confirm the radical pathway of the reaction, it was repeated in the air (absence of argon atmosphere). In these conditions, no product was obtained after 24 h.

In order to show the efficiency of present protocol, we compared our results for amidation of *p*-chlorobenzaldehyde with previously reported methods and the results are shown in Table 3. As it is evident from the results this method avoids the disadvantages of some other methods such as longer reaction time and harsh reaction conditions.

Table 3. Comparison of various catalysts for the amidation of *p*-chlorobenzaldehyde with ammonium chloride.

Entry	Yield (%)	Time	Catalyst	reference
1	89.4	4 h	Nickel peroxide	[16]
2	48	4 h	Cu_2O	[18]
3	52	6 h	MagCNTs@SiO_2–linker–CuI	[19]
4	46	5 h	$CuCl_2$	This work
4	78	40 min	Catalyst **4**	This work

Experimental section

Material and method

Melting points were measured on an Electrothermal 9100 apparatus. FT-IR spectra were determined on a Bruker Alfa FT-IR spectrometer. ^1H NMR (400 MHz) and ^{13}C NMR (100 MHz) spectra were recorded on a Bruker DRX-400 in DMSO-d_6 as solvent and TMS as an internal standard. Chemical shifts on ^{1}H and ^{13}C NMR were expressed in ppm downfield from tetramethylsilane. Elemental analyses were performed on a Carlo-Erba EA1110CNNO-S analyzer and agreed (within 0.30) with the calculated values. XRD was carried out on a Philips X-Pert diffractometer using Co tube. Scanning electron microphotographs (SEM-EDX) were obtained on a PHILIPS XL30 electron microscope. ICP analysis was accomplished using a VISTA-PRO, CCD simultaneous ICP analyzer. Magnetic properties of catalyst were obtained by vibrating sample magnetometer/Alternating Gradient Force Magnetometer (VSM/AGFM, MDK Co, Ltd, Iran). All the chemicals were purchased from Merck and used without further purification. All solvents used were dried and distilled according to standard procedures.

General procedure for the synthesis of catalyst 4

[α-Fe_2O_3@HAp-Si-$(CH_2)_3$-NH_2] was synthesized according to the references[3a,27] with a few modification and then was allowed to react with equimolar amount of 2-hydroxybenzaldehyde in super dry ethanol for 24 h under Ar atmosphere. Then, the solid product was magnetically separated by an external magnet and washed with dry ethanol to produce the catalyst **3** (Scheme 1). A stirring mixture of catalyst **3** and $CuCl_2$ in ethanol were heated at room temperature for 12 h. The resultant light brown precipitate formed was filtered, washed repeatedly with ethanol, and air-dried under vacuum at room temperature to produce catalyst **4**.

General procedure for the synthesis of amide derivatives (5a-k, 6a-e)

A mixture of ammonium chloride or aniline hydrochloride (2 mmol), aryl aldehyde (1 mmol), Na_2CO_3 (0.21 g, 2 mmol) and nanocatalyst (0.01 g, 1.4 mol%) in acetonitrile (1 mL) was stirred at room temperature. Then *tert*-butyl hydroperoxide (TBHP) (0.4 mL) was added under argon atmosphere. The reaction mixture was stirred at 50°C for 40 min. The progress of the reaction was monitored by TLC (EtOAc:*n*-hexane, 1:1). After completion of the reaction, the reaction mixture was diluted with ethyl acetate and the catalyst was easily separated by an external magnet and was washed several times with ethyl acetate. The mixed organic solvents were concentrated under vacuum to furnish the desired products (**5a-k, 6a-e**). All isolated products were identified by spectroscopic analysis (FT-IR, ^{1}H NMR and ^{13}C NMR). The spectral data and melting points of known compounds were compared with those reported in the literature.

4-Formylbenzamide (**5b**): white powder, IR (KBr) ν_{max}/cm^{-1}: 3375, 3178 (NH_2), 1664 (CONH); ^{1}H NMR (400 MHz, DMSO-d_6) δ_H: 10.09 (s, br., 1H, CHO), 8.24 (s, br., 2H, NH), 8.07 (d, *J* = 8.0 Hz, 1H), 7.98 (d, *J* = 8.0 Hz, 1H); ^{13}C NMR (100 MHz, DMSO-d_6) δ_C: 192.9, 167.6, 132.3, 129.3, 128.1, 127.3; Anal. Cald. for $C_8H_7NO_2$ (149.1): C, 64.42; H, 4.73; N, 9.39; Found: C, 64.51 ; H, 4.55 ; N, 9.20 %.

N-Phenylthiophene-2-carboxamide (**6d**): yellow powder, IR (KBr) ν_{max}/cm^{-1}: 3303 (N-H), 1633 (CONH); ^{1}H NMR (400 MHz, DMSO-d_6) δ_H: 10.23 (s, br., 1H, NH), 8.03 (d, *J* = 3.6 Hz, 1H), 7.87 (d, *J* = 5.2 Hz, 1H), 7.72 (d, *J* = 7.6 Hz, 2H), 7.36 (t, *J* = 7.6 Hz, 2H), 7.23 (dd, *J* = 5.2, 3.6 Hz, 2H), 7.12 (t, *J* = 7.2 Hz, 1H); ^{13}C NMR (100 MHz, DMSO-d6) δ_C: 159.8, 140.0, 138.7, 131.8, 129.1, 128.6, 128.0, 123.7, 120.3; Anal. Cald. for $C_{11}H_9NOS$ (203.3): C, 65.00; H, 4.46; N, 6.89; Found: C, 65.16; H, 4.35 ; N, 6.75 %.

2,4-Dichloro-*N*-phenylbenzamide (**6e**): yellow powder, IR (KBr) ν_{max}/cm^{-1}: 3342 (N-H), 1659 (CONH); ^{1}H NMR (400 MHz, DMSO-d_6) δ_H: 10.54 (s, br., 1H, NH), 7.78 (d, *J* = 2.0 Hz, 1H), 7.70 (d, *J* = 8.0 Hz, 1H), 7.64 (d, *J* = 8.0 Hz, 2H), 7.56 (dd, *J* = 8.2, 2.0 Hz, 1H), 7.35 (m, 2H), 7.13 (t, *J* = 7.4 Hz, 1H); ^{13}C NMR (100 MHz, DMSO-d_6) δ_C: 164.0, 138.8, 135.8, 134.8, 130.3, 129.2, 128.8, 128.7, 127.4, 124.0, 119.5; Anal. Cald. for $C_{13}H_9Cl_2NO$ (266.1): C, 58.67; H, 3.41; N, 5.26; Found: C, 58.77 ; H, 3.52 ; N, 5.11 %.

Conclusion

In conclusion, a novel heterogeneous HAp-encapsulated-α-Fe_2O_3-based Cu(II) organic-inorganic hybrid nanocatalyst was successfully produced and its catalytic activity was explored in the synthesis of amide derivatives from aromatic aldehydes with ammonium chloride and aniline hydrochloride in good yield and lower reaction time. The magnetic nature of this nanaocatalyst allows its easy recovery and recycling by an external magnetic field.

Acknowledgment

The authors are grateful to the Research Council of University of Guilan for the financial support of this research work.

Notes and reference

Department of Chemistry, Faculty of Sciences, University of Guilan, P. O. Box 41335-1914, Rasht, Iran. E-mail address: m-chem41@guilan.ac.ir;Tel.: (+98) 13 33770899; Fax:(+98) 13 33333262

1 Z.-L. Lu, E. Lindner and H. A. Mayer, *Chem. Rew.*, 2002, **102**, 3543-3578.

2 M. Kidwa, J. Arti and S. Bhardwaj, *Mol Divers.*, 2012, **16**, 121-128.

3 a) L. Ma'mani, M. Sheykhan, A. Heydari, M. Faraji and Y. Yamini, *Applied Catal. A*, 2010, **377**, 64-69. b) W. Teunissen, A. A. Bol and J.W. Geus, *Catal. Today*, 1999, **48**, 329–336. c) T.-J. Yoon, W. Lee, Y.-S. Oh and J.-K. Lee, *New J. Chem.*, 2003, **27**, 227–229. d) H. Yoon, S. Ko and J. Jang, *Chem. Commun.*, 2007, 1468–1470. e) H.-H. Yang, S.-Q. Zhang, X.-L. Chen, Z.-X. Zhuang, J.-G. Xu and X.-R. Wang, Anal. Chem., 2004, **76**, 1316. f) D. Lee, J. Lee, H. Lee, S. Jin, T. Hyeon and B. M. Kim, *Adv. Synth. Catal.*, 2006, **348**, 41–46. g) Y. Zhang, Z. Li, W. Sun and C. Xia, *Catal. Commun.*, 2008, **10**, 237–242. h) J. Deng, L.-P. Mo, F.-Y. Zhao, L.-L. Hou, L. Yang and Z.-H. Zhang, *Green Chem.*, 2011, **13**, 2576-2584. i) Y.-H. Liu, J. Deng, J.-W. Gao and Z.-H. Zhang, *Adv. Synth. Catal.*, 2012, **354**, 441-447.

4 a) C. Baleizão, A. Corma, H. García and A. Leyva, *Chem. Commun.*, 2003, 606–607. b) D. Wang and D. Astruc, *Chem. Rev.,* 2014, **114**, 6949-6985. c) P. D. Stevens, G. Li, J. Fan, M. Yen and Y. Gao, *Chem. Commun.*, 2005, 4435–4437. f) C. O´. Da´ laigh, S. A. Corr,

Y. Gun'ko and S. J. Connon, *Angew. Chem. Int. Ed.*, 2007, **46**, 4329–4332.

5 A. P. Wight and M. E. Davis, *Chem. Rev.*, 2002, **102**, 3589-3614.

6 V. R. Pattabiraman and J. W. Bode, *Nature*, 2011, **480**, 471-479.

7 J. W. Bode, *Curr. Opin. Drug Discov. Dev.*, 2006, **9**, 765-775.

8 C. A. G. N. Montalbetti and V. Falque, *Tetrahedron*, 2005, **61**, 10827-10852.

9 P. Starkov and T. D. Sheppard, *Org. Biomol. Chem.*, 2011, **9**, 1320-1323.

10 B. Cornils and W. A. Herrmann, *Applied Homogeneous Catalysis with Organometallic Compounds*: A Comprehensive Handbook, VCH, Weinheim, 1996.

11 a) C. Gunanathan, Y. Ben-David and D. Milstein, *Science*, 2007, **317**, 790–792, b) L. U. Nordstom, H. Vogt and R. Madsen, *J. Am. Chem. Soc.*, 2008, **130**, 17672–17673, c) S. Yaragorla, G. Singh, P. L. Saini and M. K. Reddy, *Tetrahedron lett.*, 2014, **55**, 4657-4660.

12 L.M. Jin, H. Lu, Y. Cui, C. L. Lizardi, T. N. Arzua, L. Wojtas, X. Cui and X. P. Zhang, *Chem. Sci.*, 2014, **5**, 2422-2427.

13 S. H. Cho, E. J. Yoo, I. Bae and S. Chang, *J. Am. Chem. Soc.*, 2005, **127**, 16046-16047.

14 T. A. Dineen, M. A. Zajac and A. G. Myers, *J. Am. Chem. Soc.*, 2006, **128**, 16046–16047.

15 a) We. P. Mai, G. Song, J. W. Yuan, L. R. Yang, G. C. Sun, Y. M. Xiao, P. Mao and L. B. Qu, *RSC Adv.*, 2013, **3**, 3869-3872. b) C. Roberta, P. Andrea, G. Giampaolo and L. D. Lidia, *Org. Lett.*, 2012, **14**, 5014.

16 K. Nakagawa, H. Inoue and K. Minami, *Chem. Commun.*, 1966, 17-18.

17 W. J. Yoo and C. J. Li, *J. Am. Chem. Soc.*, 2006, **128**, 13064-13065.

18 S. C. Ghosh, J. S. Y. Ngiam, A. M. Seayad, D. T. Tuan, C. L. L. Chai and A. Chen, *J. Org. Chem.*, 2012, **77**, 8007-8015.

19 D. Saberi and A. Heydari, *Appl. Organometal. Chem.*, 2013, **28**, 101-108.

20 a) M. Sheykhan, M. Mohammadquli and A. Heydari, *J. Mol. Struct.*, 2012, **1027**, 156-161, b) M. Mohsenimehr, M. Mamaghani, F. Shirini, M. Sheykhan and F. Azimian Moghaddam, *Chin. Chem. Lett.*, 2014, **25**, 1387-1391, c) L. Ma'mani, M. Sheykhan and A. Heydari, *Applied Catal. A*, 2011, **395**, 34-38, d) M. Sheykhan, L. Ma'mani, A. Ebrahimi and A. Heydari, *J. Mol. Catal. A*, 2011, **335**, 253-261.

21 S. Thomas, K. Joseph, S. K. Malhotra, K. Goda and M. S. Sreekala, Polymer Composites, Volume 2, Nanocomposites, Wiley-VCH, 2013, p 34.

22 Chemical Book, http://www.chemicalbook.com/.

23 D. R. Lide and G. W. A. Milne, Handbook of Applied Data on Organic Compounds, 3rd E.d., 1994, Vol 1, CRC Press, Inc. Boca Raton, FL.

24 J. Wang, X. Yin, J. Wu, D. Wu and Y. Pan, *Tetrahedron*, 2013, **69**, 10463-10469.

25 R. Cadoni, A. Porcheddu, G. Giacomelli and L.D. Luca, *Org. Lett.*, 2012, **14**, 5014–5017 and the references therein.

26 (a) Z. Liu, J. Zhang, S. Chen, E. Shi, Y. Xu and X. Wan, *Angew. Chem., Int. Ed.*, 2012, **51**, 3231–3235. (b) K. Xu, Y. Hu, S. Zhang, Z. Zha and Z. Wang, *Chem. Eur. J.*, 2012, **18**, 9793–9797.

27 M. Khoobi, L. Ma'mani, F. Rezazadeh, Z. Zareie and A. Foroumadi, *J. Mol. Catal. A*, 2012, **359**, 74-80.

Graphical abstract

Synthesis of copper(II) complex covalently anchoring (2-iminomethyl)phenol moiety supported on HAp-encapsulated-α-Fe_2O_3 as an inorganic–organic hybrid magnetic nanocatalyst for the synthesis of primary and secondary amides

M. Mamaghani[a,*], F. Shirini[a], M. Sheykhan[a], M. Mohsenimehr[a]

[a]Department of Chemistry, Faculty of Sciences, University of Guilan, P. O. Box 41335-1914, Rasht, Iran. E-mail address: m-chem41@guilan.ac.ir; Tel.: (+98) 13 33770899; Fax: (+98) 13 33333262